Physics Letters B 835 (2022) 137592

Contents lists available at ScienceDirect

Physics Letters B

journal homepage: www.elsevier.com/locate/physletb

Impact of parton energy loss and nPDFs on J/ψ production in proton-nucleus collisions

Li-Hua Song [a,*], Peng-Qi Wang [a], Yin-Jie Zhang [b]

[a] College of Science, North China University of Science and Technology, Tangshan 063210, PR China
[b] College of Physics Science and Technology, Hebei University, Baoding 071002, PR China

ARTICLE INFO

Article history:
Received 3 August 2022
Received in revised form 17 November 2022
Accepted 22 November 2022
Available online 24 November 2022
Editor: J. Hisano

Keywords:
Parton energy loss
Parton distribution
J/ψ production

ABSTRACT

The impact of parton energy loss and nuclear parton distribution functions (nPDFs) on J/ψ production in proton-nucleus collisions are investigated by means of the E866, LHC and RHIC experimental data. By the recent EPPS21 nPDFs, a leading order phenomenological analysis of J/ψ production cross-section ratios is performed for E866 experimental data with considering the parton energy loss effect following Landau-Pomeranchuk-Migdal (LPM) regime. The gluon transport coefficient $\hat{q}_g$ extracted from the E866 data in $0.20 < x_F < 0.65$ region is $\hat{q}_g = 0.35 \pm 0.01$ GeV^2/fm with $\chi^2/ndf = 1.01$, which indicates that the significantly better-constrained gluon distributions provided by EPPS21 contribute to accurately determining the gluon energy loss. It is founded that for E866 data in $0.20 < x_F < 0.65$ the depletion induced by $c\bar{c}$ energy loss is the largest, gluon energy loss is the second, and quark energy loss is the smallest. In addition, it can be seen that for LHC and RHIC experiment the role of nPDFs and gluon energy loss on J/ψ production are both significant, which indicates that operating more precise measurements at LHC and RHIC in the future can facilitate significantly better-constrained gluon energy loss and nPDFs.

1. Introduction

In the process of J/ψ production from proton-nucleus collisions, the cold nuclear matter effects such as nuclear parton distribution functions (nPDFs) [1–4], parton energy loss induced by the multiple scattering with propagating in QCD medium [5,6] or fully coherent energy loss (FCEL) [7], are responsible for J/ψ suppression in p-A collisions with respect to p-p collisions. The suppression of high-$p_\perp$ particles and heavy-quarkonium, which are observed in heavy-ion collisions at RHIC and LHC and proposed as a potential signal of Quark-Gluon Plasma (QGP) formation, are even induced by some of those nuclear matter effects. Hence, a solid understanding of the nuclear modification of J/ψ production in cold nuclear matter is required for quantifying the properties of the QGP created in heavy-ion collisions at LHC and RHIC.

So far, no consensus on the modification of cold nuclear matter effects responsible for J/ψ suppression has been achieved, and various mechanisms have been proposed for explaining J/ψ suppression, for example the nuclear modification due to the effective absorption cross section of the $c\bar{c}$ pair [8], the nuclear modification based on the reduction of the overlap with the J/ψ wave function induced by the increase of the $c\bar{c}$ pair invariant mass because of the multiple soft rescattering through the nucleus [9], and the nuclear modification according to parton radiative energy loss induced by multiple scattering of fast partons passing through the nucleus [10,11].

Generally speaking, the cold nuclear matter effects in the initial state of the J/ψ production process should include the incident parton energy loss induced by gluon radiation due to multiple scattering of fast partons when passing through the nucleus, as well as the correction of parton distribution functions due to the effects such as nuclear shadowing, anti-shadowing, EMC effect and Fermi motion effect in different regions of parton momentum fraction. It is now clear that a charm quark pair is produced first through the interaction of a projectile on a target parton, which contributes to J/ψ production. Hence, the finial state nuclear effects mainly include the energy loss of $c\bar{c}$ pair when traveling through the nucleus, and in the case of J/ψ produced in the target nucleus, the so-called nuclear absorption effect induced by the strong interactions between the pre-meson charm quark pair with the nuclear matter also reduces the probability of forming a high-energy J/ψ. In the present study and together with our previous works [12–14], the dominant role is played by the parton energy loss effect which follows Landau-Pomeranchuk-Migdal (LPM) regime [15,16]. Simultaneously, the correction of parton distribution functions of the target nucleus also leads to a corresponding

* Corresponding author.
E-mail address: songlh@ncst.edu.cn (L.-H. Song).

https://doi.org/10.1016/j.physletb.2022.137592

depletion of J/ψ production especially obvious for gluon shadowing of the gluon nPDF at small $x_2 < 10^{-2}$ with RHIC and LHC energies [17]. Therefore, the quantitative role of parton energy loss effect depends on the nuclear parton distribution functions of the target nucleus.

Recently, a global QCD analysis of nPDFs (EPPS21) is presented. Compared with other nPDF sets, EPPS21 nPDFs include more data from proton-lead collisions at LHC and LHCb for 5 TeV and 8 TeV, which leads to significantly better-constrained gluon distributions at small and intermediate values of the momentum fraction x [1]. By means of EPPS21 [1], the present study aims at quantitatively describing the respective role of incident quark and gluon energy loss, as well as color octet $c\bar{c}$ pair energy loss on J/ψ production for E866, LHC and RHIC experiments. The outline of this article is as follows. A brief formalism for J/ψ production in p-A collisions and the basics of parton energy loss model for J/ψ suppression are presented in section 2. In section 3, the calculations of the J/ψ production cross-section ratios with EPPS21 and parton energy loss effect are given. Finally, we draw conclusions and summaries in section 4.

2. Formalism for J/ψ production and basics for parton energy loss effect

In the process of J/ψ formation from p-A collisions, $c\bar{c}$ pair is produced first by the interaction of a projectile on a target parton, and the next is the non-perturbative formation of the colorless asymptotic state. Based on the color evaporation model (CEM) [18], the differential cross section of J/ψ production can be expressed as:

$$\frac{d\sigma}{dx_F} = \rho_{J/\psi}\int_{2m_C}^{2m_D} dm \frac{2m}{\sqrt{x_F^2 s + 4m^2}}\Big[f_g^p(x_1,m^2) f_g^A(x_2,m^2)\sigma_{gg}(m^2) + \sum_{q=u,d,s}\Big\{f_q^p(x_1,m^2) f_{\bar{q}}^A(x_2,m^2) + f_{\bar{q}}^p(x_1,m^2) f_q^A(x_2,m^2)\Big\}\sigma_{q\bar{q}}(m^2)\Big] \tag{1}$$

Here, f_i^p (f_i^A) represents the parton distribution function in the proton (nucleus) with the proton (nucleus) parton momentum fractions x_1 (x_2), $x_F = x_1 - x_2$, $m^2 = x_1 x_2 s$ ($\sqrt{s}$ denotes the center of mass energy of the hadronic collision), the charm-quark mass is $m_C = 1.3$ GeV, D meson mass is $m_D = 1.87$ GeV, and $\rho_{J/\psi}$ means the probability of $c\bar{c}$ pair producing the J/ψ particle. In addition, as the influence of next-to-leading order (NLO) processes in J/ψ production is not obvious and the form of the differential cross section ratio given by the data actually diminishes the QCD next-to-leading order correction [7,12], in this work we use the LO $c\bar{c}$ partonic production cross section from the gluon fusion (quark-antiquark annihilation). Here, $\sigma_{gg}(\sigma_{q\bar{q}})$ represents the LO $c\bar{c}$ partonic production cross section from the gluon fusion (quark-antiquark annihilation).

At initial state for J/ψ formation in p-A collisions, the incident quark and gluon undergo multiple soft collisions accompanied by gluon emission when passing through cold nuclear matter, which induces some energy ε carried away by these radiated gluons with the probability distribution $D(\varepsilon)$. In this case, due to the induced radiation of gluons with the formation time smaller than the medium length, the initial state energy loss follows LPM regime with $\langle\varepsilon\rangle_{LPM} \propto \hat{q}L^2$ [15,16]. Here, $\hat{q}$ denotes the transport coefficient and L means the passing length in the target. Baier, Dokshitzer, Mueller, Peigné and Schiff (BDMPS) have proposed the formalism suitable for describing the LPM energy loss [19,20], which can be expressed as [21,22]:

$$D(\varepsilon) = \sum_{n=0}^{\infty}\frac{1}{n!}\Big[\prod_{i=1}^{n}\int d\omega_i \frac{dI(\omega_i)}{d\omega}\Big]\delta\Big(\varepsilon - \sum_{i=1}^{n}\omega_i\Big) \times \exp\Big[-\int_0^{+\infty} d\omega \frac{dI(\omega)}{d\omega}\Big] \tag{2}$$

Here, with gluons being emitted independently, $D(\varepsilon)$ is the normalized sum of the emission probabilities for an arbitrary number of n gluons carrying away the total energy ε, and $dI(\omega)/d\omega$ is the medium-induced gluon spectrum. According to BDMPS framework, F. Arleo has derived an analytic parametrization of the probability distribution for the initial-state LPM energy loss [23]:

$$D(\varepsilon) = \frac{1}{\sqrt{2\pi}\sigma(\varepsilon/\omega_c)}\exp\Big[-\frac{(\log(\varepsilon/\omega_c) - 2\mu)^2}{2\sigma^2}\Big] \tag{3}$$

where $\omega_c = \frac{1}{2}\hat{q}L^2$, $\mu = -2.55$ and $\sigma = 0.57$ and the transport coefficient $\hat{q}$ is the free parameter adjusted to the experimental data.

At finial state for J/ψ production, the color octet $c\bar{c}$ pair also experience the medium-induced energy loss. In the light of BDMPS framework, the Salgado-Wiedemann (SW) quenching weights fitting for finial-state heavy quark energy loss are available as a FORTRAN routine [22]. If the formation time of the gluons in the induced radiation is larger than the medium length, the color octet $c\bar{c}$ pair may undergo the fully coherent energy loss (FCEL) with $\langle\varepsilon\rangle_{FCEL} \propto \frac{\sqrt{\hat{q}L}}{M}\cdot E$ (M and E respectively denote the mass and energy of the parton) [24].

In view of the medium-induced energy loss leading to the rescaling of the parton momentum fraction, the observed J/ψ with the momentum fraction x_F actually comes from the color octet $c\bar{c}$ pair originally produced at the higher value $x'_F = x_F + \Delta x_F$ with $\Delta x_F = \varepsilon_{c\bar{c}}/E_p$ (E_p means the beam energy in the rest frame of the target nucleus). Similarly, the energy loss of incident quark (gluon) brings about the rescaling of its momentum fraction from $x_{1q(g)}$ to $x'_{1q(g)}$ with $x'_{1q(g)} = x'_1 + \varepsilon_{q(g)}/E_p$ and $x'_1 = \frac{1}{2}\Big[\sqrt{(x'_F)^2(1-m^2/s)^2 + 4m^2/s} + x'_F(1-m^2/s)\Big]$. Then, in consideration of parton energy loss effect the charmonium production cross-section $d\sigma_{p-A}/dx_F$ can be modified as:

$$\frac{d\sigma_{p-A}}{dx_F}(x_F) = \int_0^{\varepsilon_{max}} d\varepsilon_{c\bar{c}} D_{c\bar{c}}(\varepsilon_{c\bar{c}}) \int_0^{\varepsilon_{max}} d\varepsilon_g D_g(\varepsilon_g) \times \int_0^{\varepsilon_{max}} d\varepsilon_q D_q(\varepsilon_q)\frac{d\sigma'}{dx_F}(\varepsilon_q,\varepsilon_g,\varepsilon_{c\bar{c}},x_F) \tag{4}$$

with

$$\frac{d\sigma'}{dx_F}(\varepsilon_q,\varepsilon_g,\varepsilon_{c\bar{c}},x_F) = \rho_{J/\psi}\int_{2m_C}^{2m_D} dm \frac{2m}{\sqrt{x'^2_F s + 4m^2}} \times [f_g^p(x'_{1g},m^2) f_g^A(x'_{2g},m^2)\sigma_{gg}(m^2) + \sum_{q=u,d,s}\{f_q^p(x'_{1q},m^2) f_{\bar{q}}^A(x'_{2q},m^2) + f_{\bar{q}}^p(x'_{1q},m^2) f_q^A(x'_{2q},m^2)\}\sigma_{q\bar{q}}(m^2)]. \tag{5}$$

Here, the upper limit on the energy loss is $\varepsilon_{max} = min(E_p - E, E)$.

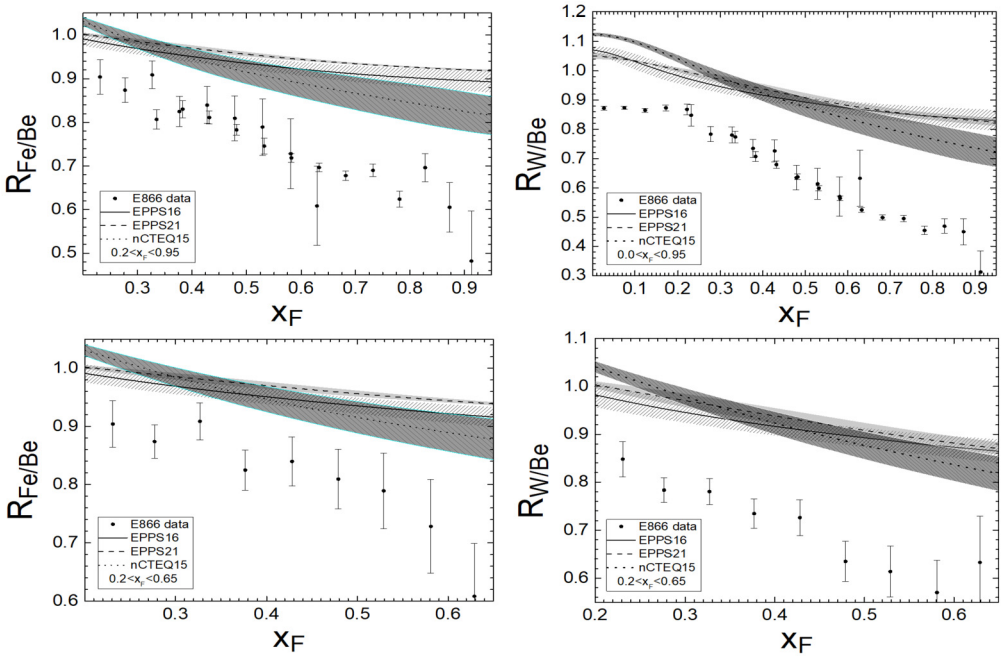

Fig. 1. The J/ψ production cross-section ratios $R_{Fe(W)/Be}(x_F)$ calculated with EPPS16 [24] (the solid lines), EPPS21 [1] (the dashed lines), nCTEQ15 [4] (the dotted lines) and the left slash bands (gray bands and black right slash bands) represent the estimated uncertainty band from the EPPS16 (EPPS21 and nCTEQ15) results. The experimental points are taken from E866 data [26,27].

3. The results with nPDFs and parton energy loss

Separately utilizing the EPPS21 [1], EPPS16 [25] and nCTEQ15 [4] nPDFs, we first investigate the quantitative role of nPDFs effect on J/ψ production for E866 [26,27], LHC [28,29] and RHIC [30] experiment. As shown in Fig. 1 and Fig. 2, the solid lines denote the results with the EPPS16, the dashed lines represent the results with the EPPS21 and the dotted lines are the calculations with the nCTEQ15. From Fig. 1 and Fig. 2, it can be seen that the modification originating from the nuclear effects of nPDFs has an obvious impact on the differential J/ψ production cross sections for E866 data, and has a huge impact for LHC and RHIC data due to the shadowing effect of gluon distributions at small values of the momentum fraction x_2. The deviation between the results obtained by the EPPS16 and EPPS21 is less than 0.02 for E866 data, and increases to about 0.1 for LHC data at $y = 3.5$ as well as RHIC data at $y = 2.5$. For LHC and RHIC data at larger y region, there is obvious deviation between the calculations with EPPS16 and EPPS21, as the EPPS21 nPDFs include more data from proton-lead collisions at LHC and LHCb for 5 TeV and 8 TeV than the EPPS16, especially for including D-meson production data [1,25,31]. In addition, for E866 and RHIC data, the trend of the curves obtained by the nCTEQ15, the EPPS21 or EPPS16 is roughly the same. However, for LHC data at large y, there is large deviation between the results with the nCTEQ15 and those with the EPPS21 (EPPS16), which may indicate that the difference methodologies between EPPS and nCTEQ groups [31–33]. The above comparison showed in Fig. 1 and Fig. 2 indicates that the EPPS21 may provide the better-constrained gluon distributions at small and intermediate x_2 than EPPS16 or nCTEQ15 due to including more data from LHC and LHCb, in spite of including data for D-meson production which may leads to overestimate the nPDFs effects for LHC data at larger y region. Furthermore, as the quantitative role of parton energy loss effect depends on nPDFs, when considering parton energy loss effect the deviation between the results severally obtained with EPPS21, EPPS16 and nCTEQ15 nPDFs should be approximately identical with the deviation between them showed in Fig. 1 and Fig. 2 (Such checks have been done). Hence, we choose EPPS21 nPDFs in the following calculation with including parton energy loss effect.

Based on the calculation scheme of parton energy loss at initial and finial state described in Section 2, by means of the latest EPPS21 [1] we investigate the quantitative role of each energy loss effect at initial and final state on J/ψ suppression for E866 [26,27], LHC [28,29] and RHIC [30] data. With $\hat{q}_q = 0.26 \pm 0.04$ GeV^2/fm [12] (obtained by the quenching weights showed as the Eq. (3) in section 2) and $\hat{q}_{c\bar{c}} = 0.29 \pm 0.07$ GeV^2/fm [34] (obtained by the SW quenching weights for heavy quarks), a leading order phenomenological analysis of J/ψ production cross-section ratios is performed for E866 experimental data and the transport coefficient $\hat{q}_g$ is the only free parameter adjusted to the data. Making use of the CERN subroutine MINUIT [35], we extract the transport coefficient $\hat{q}_g$ by fitting the E866 data in $0.20 < x_F < 0.65$ (18 data points), $0.30 < x_F < 0.95$ (26 data points), $0.20 < x_F < 0.95$ (44 data points) and $0.00 < x_F < 0.95$ (27 data points), respectively. The obtained results are summarized in Table 1. From Table 1, it can be seen that our calculations agree well with the E866 data for $0.20 < x_F < 0.65$, but do not give a good agreement with the data in $0.30 < x_F < 0.95$, $0.20 < x_F < 0.95$ or $0.00 < x_F < 0.95$ range, as other cold nuclear effects (such as gluon saturation, FCEL and nuclear absorption effects) may exist at small or large x_F. In view of the E866 experimental data in intermediate x_F ($0.20 < x_F < 0.65$) giving a relatively clean probe for the energy loss effect following LPM regime, we determine the extracted transport coefficient of gluon energy loss is $\hat{q}_g = 0.35 \pm 0.01$ GeV^2/fm ($\chi^2/ndf = 1.01$). This value is in accordance with the well-known statement that the transport coefficient of gluon is larger than that of quark owing to the ratio of the Casimir factors $C_A/C_F = 9/4$ in the leading logarithmic approximation [36]. It is worth emphasizing that the significantly better-constrained gluon distributions provided by EPPS21 contribute to better constraining the precise value of transport coefficient of gluon.

In order to directly display the quantitative role of incoming gluon, quark and outgoing $c\bar{c}$ energy loss effects on J/ψ production, by means of EPPS21 [1], the dashed, dotted, dash-dotted and solid lines in Fig. 3 and Fig. 4 separately show the results

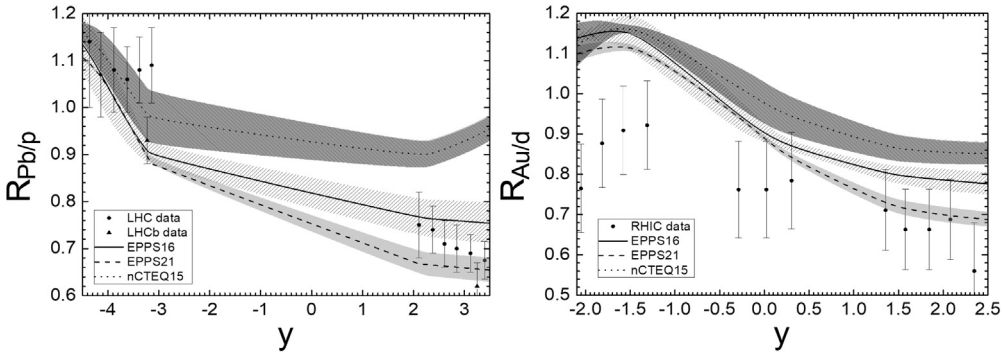

Fig. 2. The J/ψ production cross-section ratios $R_{Pb/p}(y)(R_{Au/d}(y))$. The filled circles (solid triangles) in left figure are attributed to ALICE collaboration (LHCb collaboration) at LHC [28,29], and the experimental points in right figure are taken from RHIC data [30]. Other notations are the same as those in Fig. 1.

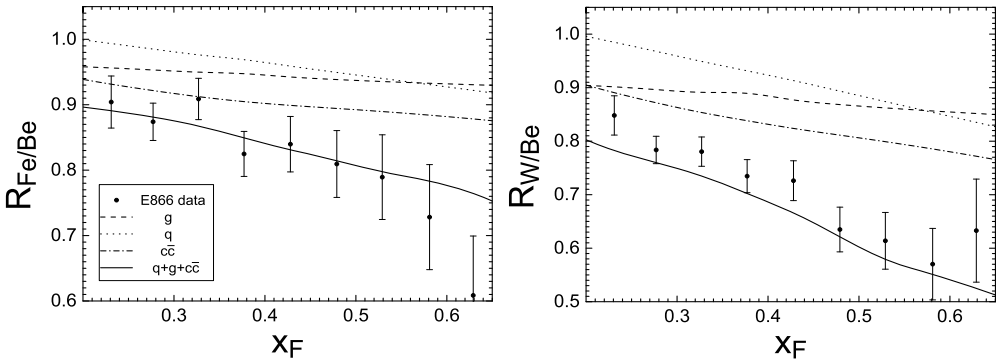

Fig. 3. The J/ψ production cross-section ratios $R_{Fe(W)/Be}(x_F)$ in $0.20 < x_F < 0.65$ obtained with EPPS21 and considering gluon energy loss (the dashed lines), quark energy loss (the dotted lines), $c\bar{c}$ energy loss (the dash-dotted lines) and together all above energy loss (the solid lines).

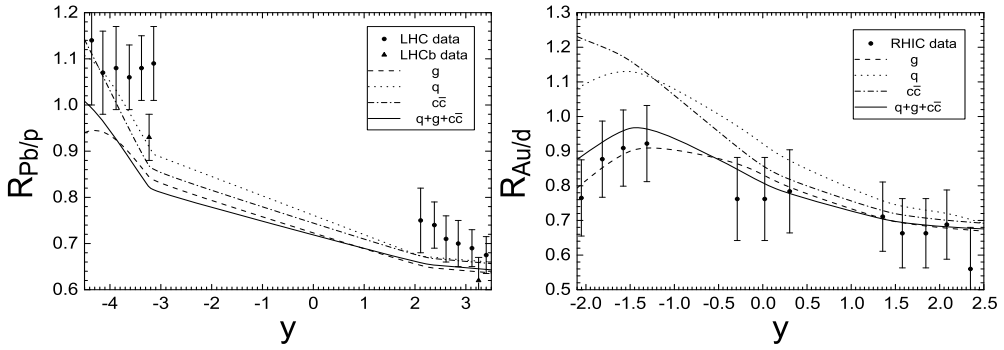

Fig. 4. The J/ψ production cross-section ratios $R_{Pb/p}(y)(R_{Au/d}(y))$ obtained with EPPS21 and considering parton energy loss effect. Other notations are the same as those in Fig. 3.

Table 1
The values of $\hat{q}_g$ and χ^2/ndf extracted from E866 data [26,27] with $\hat{q}_q = 0.26 \pm 0.04$ GeV^2/fm, $\hat{q}_{c\bar{c}} = 0.29 \pm 0.07$ GeV^2/fm and EPPS21 nPDFs.

Momentum fraction	Target	Data points	$\hat{q}_g$ (GeV^2/fm)	χ^2/ndf
$0.20 < x_F < 0.65$	W,Fe	18	0.35 ± 0.01	1.01
$0.30 < x_F < 0.95$	W,Fe	26	0.30 ± 0.02	7.54
$0.20 < x_F < 0.95$	W,Fe	44	0.27 ± 0.02	4.76
$0.00 < x_F < 0.95$	W	27	0.50 ± 0.02	16.85

with considering gluon energy loss ($\hat{q}_g = 0.35 \pm 0.01$ GeV^2/fm), quark energy loss ($\hat{q}_q = 0.26 \pm 0.04$ GeV^2/fm), $c\bar{c}$ energy loss ($\hat{q}_{c\bar{c}} = 0.29 \pm 0.07$ GeV^2/fm) and together all above energy loss. From Fig. 3, we can directly see that the role of $c\bar{c}$ energy loss effect on J/ψ suppression for E866 experiment is most significant and increases with the increase of x_F and the mass of the target. The J/ψ suppression induced by gluon energy loss is also obvious with x_F from 0.20 to 0.65, which facilitates better constraining the transport coefficient of gluon energy loss in cold nuclear matter. In addition, the depletion due to quark energy loss becomes gradually evident with the increase of x_F from 0.20 to 0.65, and the solid lines considering gluon, quark and $c\bar{c}$ energy loss effects have a good agreement with the E866 data in $0.20 < x_F < 0.65$.

By comparing Fig. 2 with Fig. 4, for LHC experiment, we can directly see that the corrections due to EPPS21 (the dashed lines in Fig. 2 left) are most significant, and the depletion of J/ψ production induced by gluon energy loss (the dashed lines in Fig. 4 left) is also significant in $-4.5 < y < 0$ region and gradually decreases with the increase of y. However, the role of the quark energy loss (the dotted lines in Fig. 4 left) or the $c\bar{c}$ energy loss (the dash-dotted lines in Fig. 4 left) on J/ψ production in LHC experiment are not obvious. It is worth noting that in the common practice of nPDF fits, the EPPS21 nPDFs already include data for D-meson production at the LHC, and assume all modifications due to the nuclear effects from nPDFs without considering parton energy loss

effects. Furthermore, the D-meson data cover quite unique kinematic region (in low x or large y range), which may lead to the nPDFs can not be well constrained by other data for this kinematic region. These may induce that the role of the parton energy loss effect on J/ψ production in LHC experiment are not obvious, especially for large y region. In addition, by comparing Fig. 2 with Fig. 4, for RHIC experiment besides the important impact of EPPS21 (the dashed lines in Fig. 2 right), it is founded that the role of gluon energy loss effect on J/ψ suppression (the dashed lines in Fig. 4 right) is most significant especially for small y region, and gradually diminishes in $1.5 < y < 2.5$ range. Nevertheless, the modification owing to the quark energy loss (the dotted lines in Fig. 4 right) or the $c\bar{c}$ energy loss (the dash-dotted lines in Fig. 4 right) is minimal, and the rescaling of the parton momentum fraction induced by the $c\bar{c}$ energy loss leads to a slight elevation in $-2.0 < y < -1.5$. Hence, it would be convincing that operating more precise measurements at LHC or RHIC in the future can facilitate significantly better-constrained nPDFs together with gluon energy loss in cold nuclear matter.

4. Summary

By means of EPPS21 and based on LPM regime, the respective role of incident quark and gluon energy loss, as well as outgoing color octet $c\bar{c}$ pair energy loss on J/ψ production at E866, LHC and RHIC experiments are investigated. A leading order phenomenological analysis of J/ψ production cross-section ratios is performed for E866 experimental data, and the transport coefficient $\hat{q}_g$ of gluon extracted from the E866 data in $0.20 < x_F < 0.65$ region is $\hat{q}_g = 0.35 \pm 0.01$ GeV^2/fm with $\chi^2/ndf = 1.01$. This value is in accordance with the well-known statement that the transport coefficient of gluon is larger than that of quark owing to the ratio of the Casimir factors $C_A/C_F = 9/4$ in the leading logarithmic approximation [36]. It is worth emphasizing that the significantly better-constrained gluon distributions provided by EPPS21 contribute to determining the precise value of transport coefficient of gluon. By comparing with the E866 experiment data, it is founded that the role of $c\bar{c}$ energy loss effect on J/ψ suppression is most significant and increases with the increase of x_F and the mass of the target, the gluon energy loss effect is always obvious with x_F from 0.20 to 0.65, the quark energy loss becomes gradually obvious with the increase of x_F from 0.20 to 0.65, and the results by considering all above energy loss have a good agreement with the E866 data in $0.20 < x_F < 0.65$. In addition, by comparing with LHC and RHIC data, it can be seen that the depletion of J/ψ production induced by gluon energy loss and the corrections of nPDFs are both significant. It is sensible that operating more precise measurements at LHC or RHIC in the future can facilitate significantly better-constrained nPDFs as well as gluon energy loss in cold nuclear matter.

Declaration of competing interest

The authors declare that they have no known competing financial interests or personal relationships that could have appeared to influence the work reported in this paper.

Data availability

Data will be made available on request.

Acknowledgements

Supported partially by National Natural Science Foundation of China (11405043), and Science and Technology Foundation of Hebei Education Department (ZD2020104).

References

[1] K.J. Eskola, et al., Eur. Phys. J. C 82 (2022) 413.
[2] R.A. Khalek, et al., J. High Energy Phys. 09 (2020) 193.
[3] A. Kusina, et al., Eur. Phys. J. C 80 (2020) 968.
[4] P. Duwentäster, et al., Phys. Rev. D 104 (2021) 094005.
[5] F. Arleo, C.-J. Naïm, S. Platchkov, J. High Energy Phys. 01 (2019) 129.
[6] L.-H. Song, L.-W. Lin, Phys. Rev. C 96 (2017) 045203.
[7] F. Arleo, G. Jackson, S. Peigné, J. High Energy Phys. 01 (2022) 164.
[8] B.Z. Kopeliovich, et al., Nucl. Phys. A 864 (2011) 203.
[9] H. Fujii, F. Gelis, R. Venugopalan, Nucl. Phys. A 780 (2006) 146.
[10] F. Arleo, F. Cougoulic, S. Peigné, J. High Energy Phys. 09 (2020) 190.
[11] L.-H. Song, W.-D. Miao, C.-G. Duan, Chin. Phys. C 38 (2014) 124103.
[12] L.-H. Song, P.-Q. Wang, Y.-J. Zhang, Chin. Phys. C 45 (2021) 041005.
[13] N. Liu, W.-D. Miao, L.-H. Song, C.-G. Duan, Phys. Lett. B 749 (2015) 88.
[14] L.-H. Song, C.-G. Duan, J. Phys. G 43 (2016) 025101.
[15] I. Helenius, et al., J. High Energy Phys. 07 (2012) 073.
[16] H. Fritzsch, Phys. Lett. B 67 (1977) 217.
[17] B.G. Zakharov, JETP Lett. 65 (1997) 615.
[18] S. Peigné, A. Smilga, Phys. Usp. 52 (2009) 659.
[19] R. Baier, et al., Nucl. Phys. B 484 (1997) 265.
[20] R. Baier, et al., J. High Energy Phys. 09 (2001) 033.
[21] C.A. Salgado, U.A. Wiedemann, Phys. Rev. D 68 (2003) 014008.
[22] C.A. Salgado, U.A. Wiedemann, Phys. Rev. Lett. 89 (2002) 092303.
[23] F. Arleo, J. High Energy Phys. 11 (2002) 044.
[24] S. Peigné, F. Arleo, R. Kolevatov, Phys. Rev. D 93 (2016) 014006.
[25] K.J. Eskola, et al., Eur. Phys. J. C 77 (2017) 163.
[26] M.J. Leitch, et al., E866/NuSea Collaboration, Phys. Rev. Lett. 84 (2000) 3256.
[27] W.M. Lee, Ph.D. Thesis, Georgia State University, 1999.
[28] B.B. Abelev, et al., ALICE Collaboration, J. High Energy Phys. 02 (2014) 073.
[29] R. Aaij, et al., LHCb Collaboration, J. High Energy Phys. 02 (2014) 072.
[30] A. Adare, et al., PHENIX Collaboration, Phys. Rev. Lett. 107 (2011) 142301.
[31] K.J. Eskola, et al., J. High Energy Phys. 05 (2020) 037.
[32] P. Duwentäster, et al., Phys. Rev. D 105 (2022) 114043.
[33] A. Kusina, et al., Phys. Rev. Lett. 121 (2018) 052004.
[34] L.-H. Song, L.-W. Lin, Y. Liu, Nucl. Sci. Tech. 29 (2018) 159.
[35] B.F. James, CERN Program Library Long Writeup D506, ftp://asis01.cern.ch/.
[36] S. Peigné, A.V. Smilga, Phys. Usp. 52 (2009) 659.